RL-556
7-13-72
011075

FURTHER STUDIES OF BACKSCATTERING FROM A FINITE CONE*

Thomas B. A. Senior
Radiation Laboratory
The University of Michigan
Ann Arbor, Michigan 48105

and

Piergiorgio L. E. Uslenghi
Department of Information Engineering
University of Illinois at Chicago Circle
Chicago, Illinois 60680

Abstract

Certain errors in the second-order contributions to the scattered field derived in an earlier study are pointed out and the corrected formulae are presented. The results are compared with experimental data and an explanation is suggested for the remaining small discrepancies.

1. Introduction

In a recent paper (Senior and Uslenghi, 1971; hereinafter referred to as [A]) the geometrical theory of diffraction was used to obtain the second-order contribution to the diffracted field in a situation which was essentially vectorial in nature. In the particular case of backscattering from a finite cone, migratory ray paths were discovered and their contributions determined. However, as pointed out by Burnside and Peters (1972), all these second-order results are in error by a factor 2 through a failure to consider the reduction of the effective strength of surface rays which strike a singularity at grazing incidence. The necessity for this correction was originally noted by Kouyoumjian (1965).

There is, in addition, an error associated only with the migratory rays.

*This research was sponsored by the Air Force Office of Scientific Research, U.S. Air Force Systems Command, under Grants AFOSR-72-2262 and 2263.

This is discussed and the corrected formulae presented. Although the agreement with experiment is now improved, there remains a small but systematic discrepancy whose nature is explored.

2. Second-order contributions

A perfectly conducting right circular cone of half-angle γ and base radius a is illuminated by a plane wave whose direction of propagation forms the angle Φ with the cone axis. We separately consider the two cases in which either the electric or the magnetic field vector is perpendicular to the plane formed by the direction of incidence and the cone axis, and define the corresponding backscattered far field coefficients S_E and S_H as in [A]. Attention will be focused on the second-order contributions to S_E and S_H, which arise from rays diffracted across the base of the cone either in the plane of incidence or via the migratory ray paths.

As previously noted, all second-order contributions in [A] must be multiplied by a factor $1/2$. This correction is required for axial as well as oblique incidence, and thus the axial formula in the classical paper by Keller (1960) contains the same error. In the limiting case of a circular disk, however, optical rays propagate on both faces; the correction factor $1/2$ applies to every ray, but since the contributions of corresponding rays on the two sides are equal, we may neglect the factor $1/2$ and consider propagation over one side only (Knott et al., 1971). In the limit $\gamma \longrightarrow \pi/2$ as the cone becomes a disk, our second-order contribution is now one half that for a disk. This clearly shows that a tip-base interaction must be included in any second-order treatment of very wide-angle cones, even though such interaction is believed negligible for small-angle cones.

Turning now to migratory rays, their contribution to H-polarization was omitted. It can be obtained by an analysis similar to the one for E-polarization and is found to differ from the latter only by a factor $\tan^2 \Phi$. This added contribution is not therefore singular on the axial caustic and its magnitude is relatively insignificant for small Φ.

As a result of these corrections, systematically applied to the formulae in [A], the caustically-corrected expression for the second-order contribution to S_E is found to be:

$$S_E^{II} = -\frac{1}{2}\left[\frac{ka}{\pi}(1+\sin^2\Phi)\right]^{1/2}\cos^2\Phi \cdot$$
$$\cdot \exp\left[2ika(1+\sin^2\Phi)^{1/2} - i\frac{\pi}{4}\right] \cdot$$
$$\cdot E(\Phi) M^* \left\{\frac{1}{2}(ka)^{1/2}\sin\Phi\right\} , \qquad (1)$$

c. f. equation (57) in [A]. The analogous expression for H-polarization is

$$S_H^{II} = \frac{1}{2}\left(\frac{ka}{\pi}\right)^{1/2} \exp(2ika - i\frac{\pi}{4})\, G(\Phi)\, M\left\{\frac{1}{2}(ka)^{1/2}\sin\Phi\right\} + S_E^{II}\tan^2\Phi , \qquad (2)$$

c. f. equation (56) in [A], where S_E^{II} is given by (1). The functions E, G and M are as defined in [A], and the asterisk denotes the complex conjugate.

3. Experimental Comparison and Discussion

The backscattered field through second order is obtained by adding the corrected expressions of the previous section to the first order contributions given in [A] (note that the signs of the last term in equation (51) are misprinted and should be reversed). The normalized cross-sections deduced from this are compared with the experimental data of [A] in Figs. 1 and 2; the treatment of the angular region outside the backward cone ($\Phi > \gamma$) is as discussed in [A].

Although the agreement between theory and experiment is somewhat improved over that displayed in Figs. 5 and 7 of [A], there is still some discrepancy, which is more clearly evident in the comparison of the axial backscattering as a function of frequency (Fig. 3). The theoretical curve parallels the experimental data over the range $8 < ka < 12$, but lies consistently 1.8 db below. In order to pinpoint the source of this discrepancy, the experimental measurements were repeated with a piece of absorber on the base of the cone, to suppress the second and higher order contributions. These data are included in Fig. 3, and although there is some scatter in the measured values, the points are aligned almost parallel to the first-order GTD prediction, which is now about 2 db below. Whatever mechanism is responsible for the discrepancy therefore applies equally to first and second-order approximations. We have also compared theory with experiment for other ranges of ka, and whereas the discrepancy is of order 1 db for ka near 2, it has risen to as much as 2.2 db for ka near 20. Thus, increasing ka does not improve the agreement between theory and experiment in the manner to be expected of an asymptotic theory.

A possible explanation of the discrepancy is the influence of the conical surface on the effective strength of the rays incident on and backscattered from the edge of the base. Computed data for the fields on the surface of a semi-infinite cone (Senior and Wilcox, 1967) show a behavior which, at large distances from the tip, can be approximated by a Fresnel integral with argument $\tau = \left(ka \tan \frac{\gamma}{2}\right)^{1/2}$. For $\tau \gg 1$, the computed results agree with physical optics, but for $\tau \approx 1.5$ can exceed physical optics by more than 1.5 db. Based on this explanation, the discrepancy between theory and experiment for axial backscatter from a finite cone is expected to increase up to $ka \cong 18$, and only then to decrease.

The modification in the strength of the field to which the rim of the base is exposed is a function of the angle between the incident ray and the nearest generator of the cone. Therefore, for off-axial incidence the various elements of the rim will be differentially affected, and for any given Φ the effect may be to either increase or decrease the backscattering with respect to the GTD prediction. This is consistent with the discrepancies visible in Figs. 1 and 2.

References

Burnside, W. D., and L. Peter, Jr. (1972), Axial radar cross section of finite cones by the equivalent current concept with higher order diffraction, Radio Science, 7, in press.

Keller, J. B. (1960), Backscattering by a finite cone, IRE Trans. Antennas Propagat., 8, 175-182.

Knott, E. F., T. B. A. Senior and P. L. E. Uslenghi (1971), High-frequency backscattering from a metallic disk, Proc. IEE (London), 118, 1736-1742.

Kouyoumjian, R. G. (1965), Asymptotic high-frequency methods, Proc. IEEE, 53, 864-876.

Senior, T. B. A., and P. L. E. Uslenghi (1971), High-frequency backscattering from a finite cone, Radio Science, 6, 393-406.

Senior, T. B. A., and P. H. Wilcox (1967), Traveling waves in relation to the surface fields on a semi-infinite cone, Radio Science, 2, 479-487.

Legends for Figures

Fig. 1. Comparison of the second order theory (curve formed by the X's and dots) with experiment (continuous line) for ka = 9.641 and $\gamma = 15^{o}$. H polarization is shown on the left and E polarization on the right.

Fig. 2. Comparison of the second order theory (curve formed by the X's and dots) with experiment (continuous line) for ka = 11.527 and $\gamma = 15^{o}$. H polarization is shown on the left and E polarization on the right.

Fig. 3. Comparison of theory and experiment for axial incidence with $\gamma = 15^{o}$. The broken line is the curve from the first order theory and the continuous line is the second order result. The measured values are shown by X's and the effect of placing absorber on the base of cone is indicated by the dots.

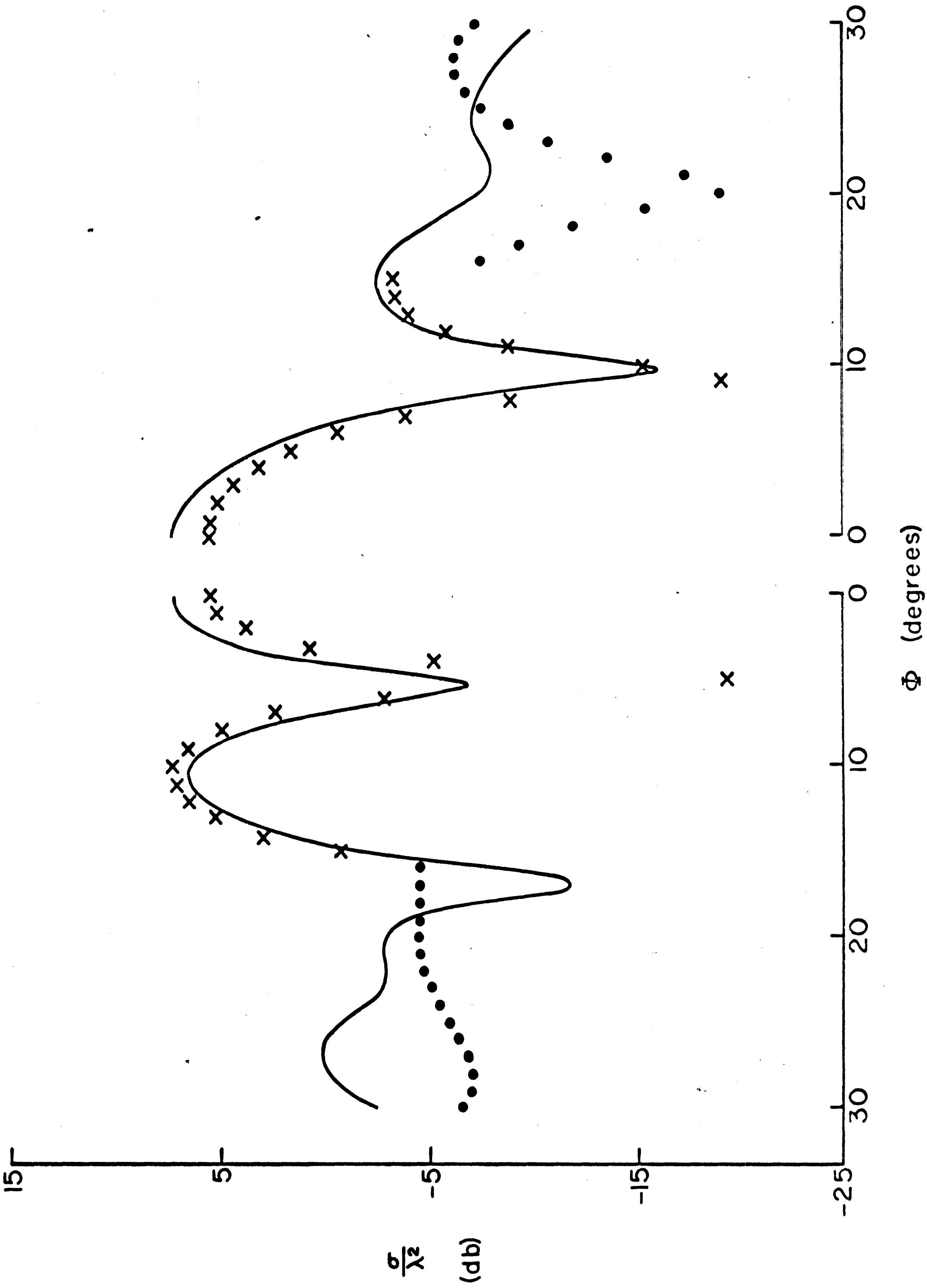

Fig. 1. Comparison of the second order theory (curve formed by the X's and dots) with experiment (continuous line) for ka = 9.641 and $\gamma = 15^{\circ}$. H polarization is shown on the left and E polarization on the right.

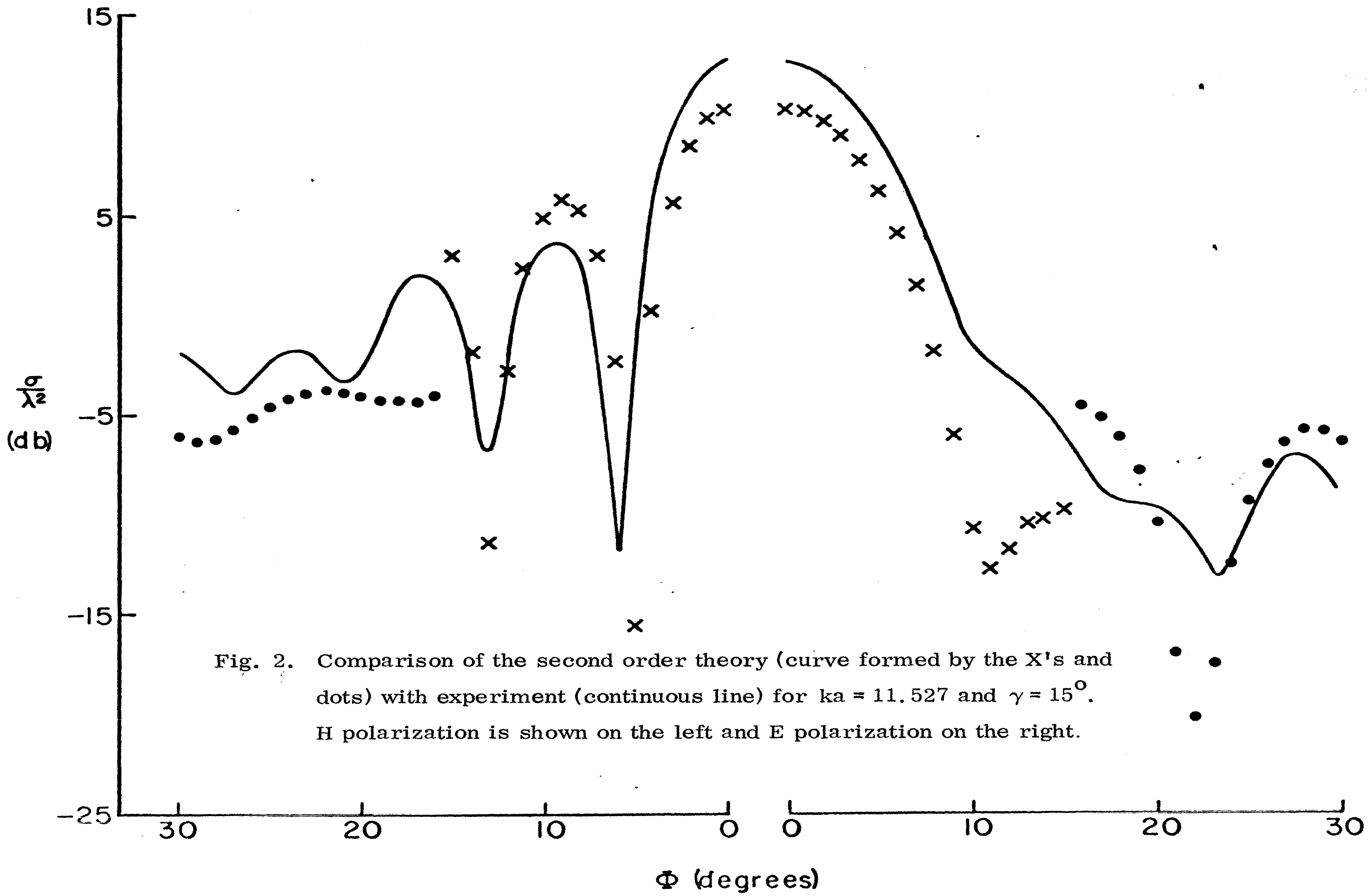

Fig. 2. Comparison of the second order theory (curve formed by the X's and dots) with experiment (continuous line) for ka = 11.527 and $\gamma = 15^{\circ}$. H polarization is shown on the left and E polarization on the right.

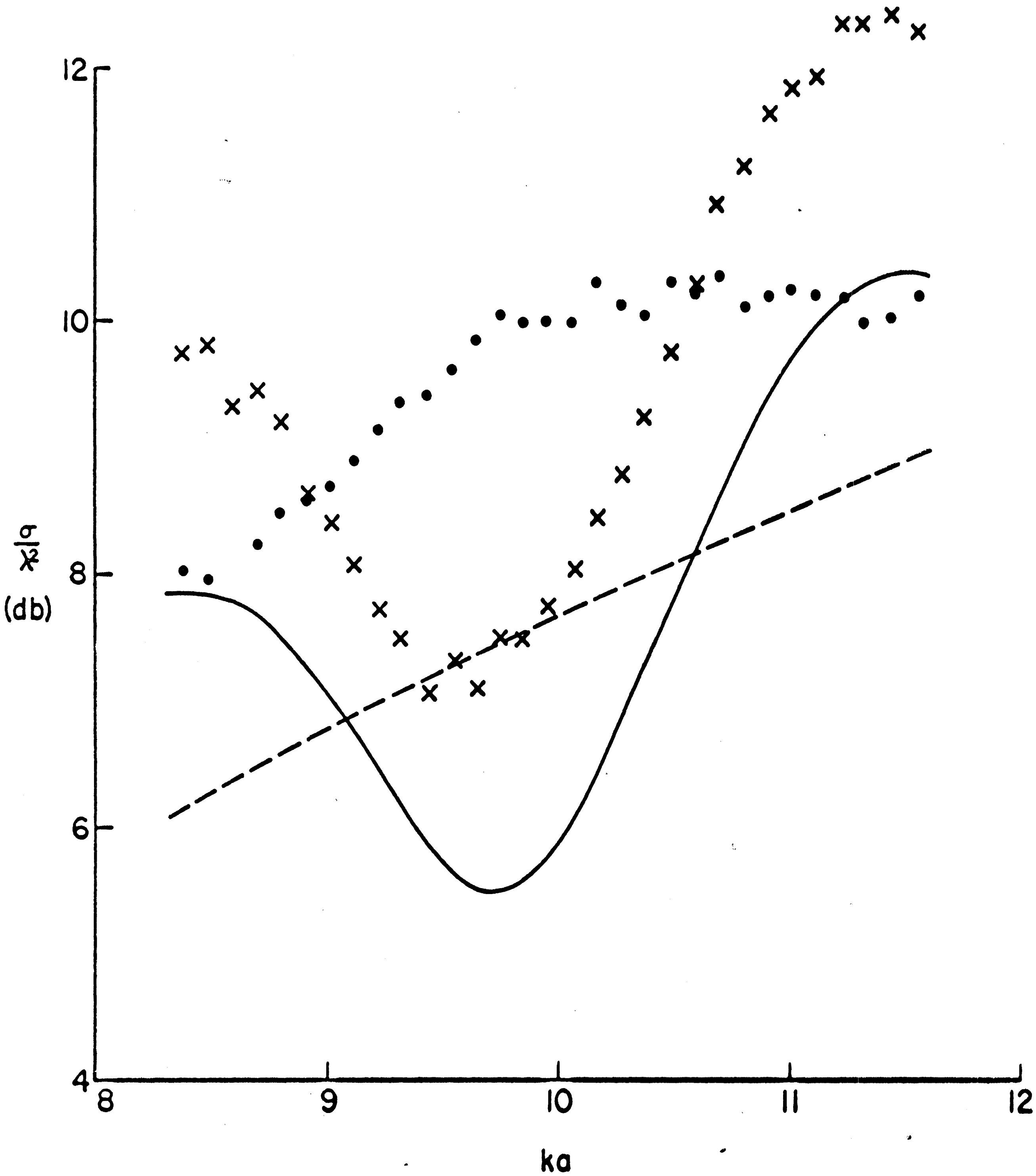

Fig. 3. Comparison of theory and experiment for axial incidence with $\gamma = 15^o$. The broken line is the curve from the first order theory and the continuous line is the second order result. The measured values are shown by X's and the effect of placing absorber on the base of the cone is indicated by the dots.